JOURNAL OF MATERIALS SCIENCE 19 (1984) 2336–2352

Magnesium diffusion, surface segregation and oxidation in Al–Mg alloys

C. LEA, C. MOLINARI*
Division of Materials Applications, National Physical Laboratory, Teddington, Middlesex, UK

Auger electron spectroscopy (AES) has been used to follow the surface segregation behaviour of magnesium at the surface of Al–Mg alloys in the temperature range up to 600° C as a function of time. The evaporation rate of magnesium from the magnesium-rich surface has also been measured. The combination of the competing processes of segregation and evaporation has been treated theoretically and compared with the experimental measurements. The measured equilibrium surface enrichment of magnesium fell from a factor of 24 at 100° C to 12 at 200° C. At higher temperature the evaporation rate exceeded the segregation rate and the surface layer became magnesium-depleted. The data also lead to a low-temperature determination of the diffusivity of magnesium in aluminium. The same Al–Mg alloys have been heat-treated, within a similar time–temperature regime, in air. The oxide films have been composition–depth profiled using AES with ion sputtering, and measurements of the rate of oxide growth lead to information about the diffusivity of magnesium through the oxide films.

1. Introduction

Undesirable effects such as tool wear, poor adhesion of applied organic films, staining, etc., occur during the fabrication of Al–Mg alloys. They are all related to changes in the composition and structure of the metal surface occurring during production heat treatments. In general, if such alloys are heated in vacuum, magnesium is depleted from the surface layer because of its surface activity and more ready evaporation, while if heated in air, the oxidation of magnesium is energetically preferred, producing a magnesium-rich oxide and consequently again, the possibility of a magnesium-depleted surface layer of the alloy. Besides the commercial implications, the behaviour of the surfaces of Al–Mg alloys is of particular interest since the two pure metals have such different evaporation rates in vacuum while, in air, they follow different oxidation rate laws.

This paper concerns the kinetics of diffusion of magnesium in Al–Mg alloys, through the lattice and the grain boundaries, to segregate at free surfaces. The kinetics of surface segregation vary as the magnesium-rich surfaces are allowed to oxidize or the magnesium is allowed to evaporate.

The nature of the surface composition and structure of Al–Mg alloys, rolled and heat treated in air, and their importance in subsequent fabrication has recently been treated elsewhere [1]. In that work the oxidation was considered of the alloys in their production, as-rolled state. In this complementary work, the segregation, evaporation and oxidation kinetics have been measured under precisely defined conditions and surface state. In this way an understanding of the precise physical laws which govern the behaviour of the alloys will be achieved enabling optimum procedures to be defined within industrial practice.

2. Materials

Two Al–Mg alloys have been used, nominally to the Aluminium Association specifications 5657

*On leave of absence from Laboratoire de Thermodynamique et Physico-Chimie Metallurgiques, ENSEEG Domaine Universitaire, St Martin d'Hères, France. Present address: Centre de Recherches Tréfimetaux, rue Michel Carré, Argenteuil, France.

0022–2461/84 $03.00 + .12

TABLE I Composition of the alloys (wt %)

Alloy	Al	Mg	Zn	Cu	Fe	Si	Mn	total others
5657	bal.	0.76	0.02	0.04	0.10	0.10	0.0035	< 0.05
5252	bal.	2.41	0.02	0.07	0.10	0.10	0.0055	< 0.05

and 5252 with 0.8 and 2.5 wt% magnesium, respectively. The analyses of the alloys is given in Table I.

The materials were in the form of 0.5 mm thick sheet, cold rolled and annealed with nominal UTS values of 215 and 235 MPa, respectively, for the low and high magnesium compositions. Coupons of about 1 cm^2 were cut and polished with emery paper followed by diamond down to 0.25 μm and ultrasonically cleaned in ethyl alcohol. The sample microstructure was examined by similar polishing of transversely mounted material with an etch in 17% HNO_3–3% HF acid solution to produce grain contrast. A typical microstructure exhibited an average grain size of 50 μm.

3. Auger electron spectroscopy

Auger electron spectroscopy (AES) enables analysis of a surface layer between about two and ten atoms thick, depending upon the inelastic mean free path (imfp) of the characteristic Auger electrons emitted. When used in conjunction with argon ion sputtering which strips off surface atom layers during the analysis, composition–depth profiles through the surface region can be built up. Both the peak intensities and the peak energies of the Auger electron spectra of aluminium and magnesium are sensitive to chemical environment and the peaks representative of the metals are clearly different from those of their oxides. As a measure of the relative quantities of aluminium and alumina, the $L_{23}VV$ Auger lines at 68 and 52 eV, respectively, could be used, but these peaks, having very low imfps [2] are very sensitive to surface contamination and the initial stages of oxide film formation. The determination of the relative amounts of aluminium and alumina from the high energy KL_2L_2 Auger lines at 1396 and 1378 eV, respectively, is more difficult because of the overlap of the associated plasmon peaks, but is less sensitive to contaminants adsorbing during the analysis because the analysis is averaged over some seven atom layers instead of two. In general, therefore, the high energy Auger lines have been used. For magnesium and magnesia the corresponding KL_2L_2 Auger lines occur at 1186 and 1174 eV, respectively.

Auger electron spectra were obtained with a 10 μm diameter 3 keV electron probe across a matrix of points on the sample surface. A relatively small probe was used to obtain a large number of spectra from each sample rather than a defocused probe, in order to negate effects of local topography. By scanning the probe, a low-resolution scanning electron micrograph could be obtained which could be used to later identify the analysed area after removal of the sample from the spectrometer, in a scanning electron or optical microscope. Composition–depth profiles were obtained by combining the AES analysis with sputtering of the sample surface using a 3 keV argon ion beam, rastered across the sample surface, with a dynamic argon pressure of 5 mPa.

Quantification of the Auger electron spectra was effected through the use of spectra from samples of pure aluminium and magnesium ion etched *in situ* and of thick oxide films of Al_2O_3 and MgO grown on these standard samples. Spectra were translated into atomic % according to standard quantification procedures. For magnesium adsorbed at the surface of alumina as a monolayer segregant the area coverage of magnesium is given by [3]

$$\phi_{Mg} = Q_{MgAl} \frac{I_{Mg}/I^{\infty}_{Mg}}{I_{Al}/I^{\infty}_{Al}} \quad (1)$$

where

$$Q_{MgAl} = \frac{\lambda_{Mg}(E_{Mg}) \cos\theta}{a_{Mg}} \left[\frac{1 + r_{Mg}(E_{Mg})}{1 + r_{Al}(E_{Mg})}\right] \quad (2)$$

In this equation $\lambda(E)$ is the imfp which is given empirically by [2]

$$\lambda(E) = \frac{538}{E^2} + 0.41(aE)^{1/2} \text{ monolayers} \quad (3)$$

E is the energy of the Auger electrons, a the atomic size defined by

$$a^3 = \frac{\text{atomic weight}}{\text{Avogadro's number} \times \text{density}}$$

here equal to 0.285 nm for magnesium, and θ is the

angle of emission of the Auger electrons from the surface normal. The $r(E)$ are backscattering factors which arise to account for the Auger electron signal from backscattering processes. I_{Al} and I_{Mg} are the measured peak intensities from the sample surface and I^{∞}_{Al} and I^{∞}_{Mg} the relative standard intensities from pure samples of the bulk elements.

In the case under consideration here, the bulk material contains a significant amount of magnesium, so that although segregated magnesium will adsorb at the free surface atomic layer, there will be a magnesium concentration in the underlying layers at equilibrium with the bulk. This must be taken into account when quantifying the spectra.

If the sample can be considered to be homogeneous to a depth greater than the imfp an equation analogous to Equation 1 may be derived [3]

$$\frac{X_{Mg}}{X_{Al}} = F_{MgAl}\frac{I_{Mg}/I^{\infty}_{Mg}}{I_{Al}/I^{\infty}_{Al}} \tag{4}$$

The absolute imfp is no longer a requisite and the matrix factor is given by

$$F_{MgAl} = \left[\frac{1+r_{Mg}(E_{Mg})}{1+r_{Al}(E_{Mg})}\right]\left[\frac{a_{Mg}}{a_{Al}}\right]^{1.5} \tag{5}$$

where the symbols are as before. Backscattering values have been taken from the Monto Carlo calculations of Ichimura and Shimizu [4].

By using these procedures it is possible to quantify accurately the spectra in terms of at% and to average the analysis over a large number of points across the sample surface.

4. Heat-treatment in vacuum

4.1. Time dependence of magnesium segregation

The solution of the diffusion equation for solute segregation to a free surface of a dilute binary alloy gives the surface concentration of solute C^t_s (atoms m^{-3}) after a time, t, as [5]

$$\frac{C^t_s - C^0_s}{C_\infty - C^0_s} = \alpha\left[1 - \exp\frac{Dt}{\alpha^2 d^2}\,\mathrm{erfc}\left(\frac{Dt}{\alpha^2 d^2}\right)^{1/2}\right] \tag{6}$$

where C_∞, asssumed constant, is the bulk solute content (atoms m^{-3}) away from the surface, D is the solute lattice diffusion coefficient ($m^2\,sec^{-1}$) and d (m) is the solute monolayer thickness at the surface, taken as the atomic size. The surface concentration of solute at time t, C^t_s, is related to the time varying bulk solute content immediately below the surface, $C^t_{z=0}$, by α, the surface enrichment ratio. This is the ratio of the concentration of segregant atoms at the surface to that in the bulk. At equilibrium $C^{\infty}_{z=0} = C_\infty$ and hence $C^{\infty}_s = \alpha C_\infty$. This time dependence of C^t_s (plotted, for universal application, as a function of $Dt/\alpha^2 d^2$) is shown in the $V = 0$ curve of Fig. 1.

From Fig. 1 it can be seen that C^t_s reaches 90% of its equilibrium value after a time $t_{90} \simeq 30\alpha^2 d^2/D$. From measurements which will be described later, for the Al–0.8Mg alloy, t_{90} ranges from about 800 h at 100° C to 1 msec at 600° C.

In general, when a binary alloy is heated in vacuum one or other of the components will preferentially deplete by evaporation. Over the temperature range of interest here, the vapour pressure of magnesium is more than nine orders of magnitude greater than that of aluminium. Hence magnesium will evaporate, limiting the rate of build-up of its surface enrichment. The effect of evaporation on the kinetics of surface segregation may be evaluated [5] as the difference between the rate of diffusion from the atom layer just below the surface and the rate of evaporation, R (atoms $m^{-2}\,sec^{-1}$)

$$d\frac{\partial C^t_s}{\partial t} = D\left|\frac{\partial C^t_z}{\partial z}\right|_{z\to 0} - R \tag{7}$$

This assumes that evaporation of the aluminium is negligible and that, since the chemical potential of the magnesium just above the surface is equal to that just below the surface, by applying Raoult's law, the rate of evaporation is proportional to the bulk solute content in the atom layer under the surface, namely $C^t_{z=0}$.

The rate of evaporation, R, may conveniently be expressed in terms of a dimensionless parameter, V, such that

$$R = \frac{VDC^t_{z=0}}{\alpha^2 d}\ \text{atoms}\,m^{-2}\,sec^{-1} \tag{8}$$

The predicted effect of varying V on the kinetics of surface segregation is shown in Fig. 1. With evaporation, the segregation level passes through a maximum before falling asymptotically to zero as a result of competition between the two mechanisms of a diffusion-limited segregation rate from a depleted zone and an evaporation rate dependent upon the segregation level. By expressing R as in Equation 8 the set of curves in Fig. 1 has universal applicability.

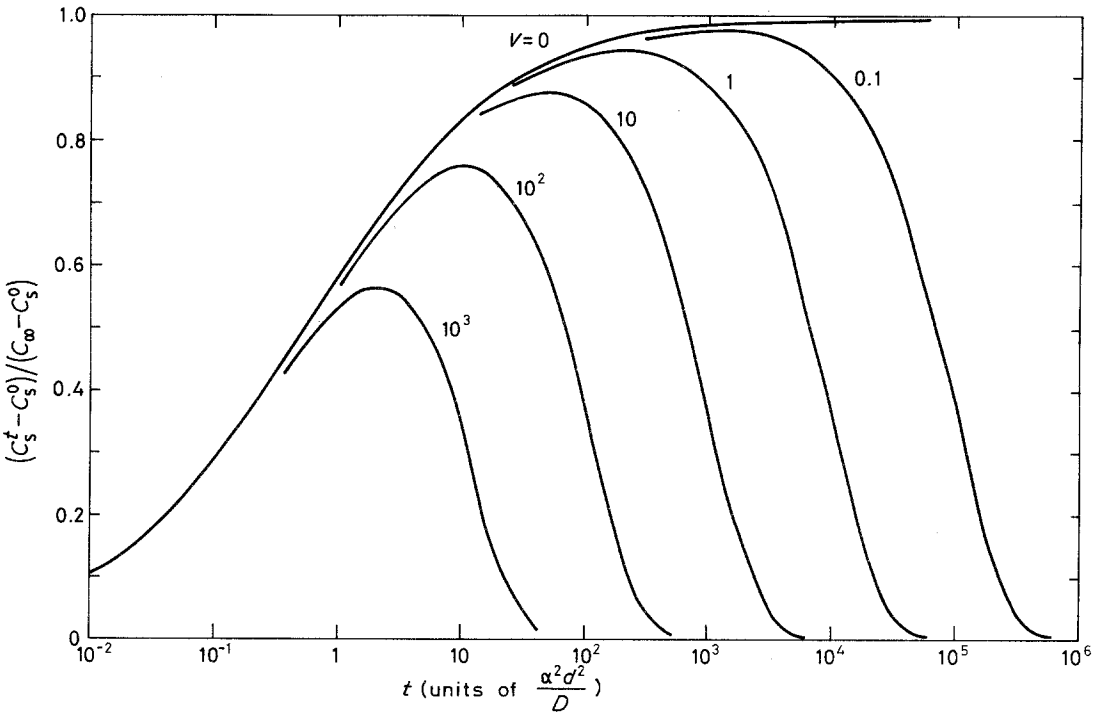

Figure 1 The time dependence of the segregation level at a free surface in vacuum for a series of evaporation rates (after Lea and Seah [5]).

4.2. Rates of evaporation

In order to test the curves of Fig. 1 it is necessary either to measure V experimentally or to describe it from thermodynamic data. Experimental measurements are described in Section 4.4.

The equilibrium vapour pressure, p, of a dilute solute, here magnesium, more volatile than its matrix is related to the vapour pressure of pure solute, p_0, by

$$p = p_0 \exp\left(\frac{\Delta G}{RT}\right)$$

where ΔG is the free energy difference between the solute in the dilute alloy and in the pure bulk state, at temperature T. To a first approximation p varies as the solute content below the surface, assuming Raoult's law is obeyed:

$$p \simeq p_0 C^{\infty}_{z=0}$$

If p is expressed in Pa, the rate of evaporation of solute from the surface is [6]

$$R = 2.64 \times 10^{24} p/(wT)^{1/2} \text{ atoms m}^{-2} \text{ sec}^{-1} \quad (9)$$

where w is the atomic weight of the solute. By combining Equations 8 and 9 the temperature dependence of V may be determined, enabling comparison of Fig. 1 with experimental measurement.

4.3. Experimental procedures

Specimen coupons, polished and cleaned were, in turn, mounted to form one face of a hollow cube constructed from the same Al–Mg alloy as the specimen, itself attached to a universal motion device within the vacuum system of the Auger electron spectrometer. The hollow cube surrounded a directly heated tungsten coil of sufficient wattage to enable the Al–Mg specimen to attain temperatures in excess of 600° C by radiation from the coil. Temperatures were monitored using a 40 μm diameter chromel–alumel thermocouple fixed to the outer surface of the sample. The temperature was controlled by the thermocouple to better than ± 3° C at equilibrium by switching only a small part of the coil current. Initially, heat was applied to the specimen holder at maximum power in order to raise the sample temperature as rapidly as possible to that required. The time taken to reach 200° C was about 30 sec and to 600° C about 3 min. Auger electron analyses were possible at elevated temperatures without distortion of the spectra.

To measure the rate of evaporation from the specimen surface and to identify any species evaporating as well as the magnesium, a copper flag was mounted a short distance from the experimental surface of the sample. This flag was one end of a rod which formed a direct vacuum feedthrough, and its end outside the vacuum chamber could be cooled using liquid nitrogen. This increased the sticking probability of evaporating species on the copper flag to close to unity. The copper rod, mounted on a wobble stick, could, by suitable adjustment, be moved such that the flag could be both ion sputtered clean and surface analysed by AES.

The experimental procedure was to clean by ion sputtering, first the cooled copper flag and then the Al–Mg sample. In the latter case the ion beam was rastered to increase the area of sputtering and so reduce the possibility of surface diffusion of mobile species from unsputtered parts of the sample surface into the cleaned area during the heat treatment. Sufficient surface atom layers were always sputtered from the sample to ensure that the bulk composition had been reached; the effect of depletion layers below the surface can affect the segregation kinetics significantly [5]. The cleanliness of the copper flag and the specimen were monitored by AES prior to any heating.

The sample was then raised to a selected temperature as quickly as possible and the composition of the surface monitored by AES as a function of time. The spectra were quantified by the procedures described in Section 3 and the composition of the surface atom layer expressed, as C_s^t, in atoms m^{-3}. Finally, the copper flag was moved in front of the Auger electron analyser and the amount of evaporated material quantified from the spectra.

4.4. Measurement of evaporation rates

The Auger electron spectra from the copper flag exhibited only copper and magnesium over the entire temperature range up to 600° C. No aluminium or contaminants were observed. In order to make quantitative measurements from the spectra, Auger peaks from both copper and magnesium were necessary. Hence for a given geometry of the Al–Mg specimen and the copper flag and a given time of heating, upper and lower limits of measurement of evaporation rate are defined; the former by the thickness of a magnesium layer on the flag equal to the ifmp of the copper high-energy Auger peak, namely about 6 atomic layers, and the latter by the detectability limit of magnesium on copper, namely about 2% monolayer. The separation and subtended angle of the flag to the specimen was well defined and known. The main source of uncertainty was probably the surface temperature inhomogeneity of the sample. It has been assumed that there was no temperature differential across the sample surface.

The measurements of the evaporation rate, R, by this method are shown in Fig. 2 for the Al–0.8Mg alloy as a function of temperature. These were only possible, within sensible times, in the temperature range 200 to 500° C. The solid curve is a plot of Equation 9 using standard vapour pressure data [7]. It can be seen that the general trend of measurements is as expected and that all the individual measurements are within an order of magnitude the theoretical line.

From the experimental measurements of R and Equation 8 it is possible to derive values for the evaporation parameter V and hence deduce the ranges of time and temperature that are applicable in Fig. 1. Values for α and for D are those obtained and discussed in later sections, but are called upon here in order to advance the argument. In the temperature range of interest, 150 to 600° C the range of V is from 1 to 100, which thus defines the limits of consideration of Fig. 1.

The significance of V in relation to Fig. 1 is best illustrated by specific examples. For a specimen temperature of 150° C, V is about 2 and $\alpha^2 d^2/D$ takes a value about 1000 sec for the Al–0.8Mg alloy. Hence, at 150° C the surface segregation level of magnesium is predicted to rise to 90% of its theoretical equilibrium value (in the absence of evaporation) in about 10 h but rise very little more before falling again below 90% C_∞ after about 160 h. Evaporation of magnesium at this temperature is very slow and the segregation level is predicted to fall to 50% C_∞ only after some 50 days.

At the upper end of our investigated temperature range, namely 600° C, the kinetics are by contrast very rapid, but the evaporation rate beats the diffusional supply of magnesium to the surface. At this temperature V is about 75 and $\alpha^2 d^2/D$ about 40 μsec. Thus, the segregation level at the free surface of the specimen, C_s^t is predicted to peak at about 0.8 C_∞ before falling rapidly to zero. The segregation level however rises to this peak value and then falls below the detection limit of

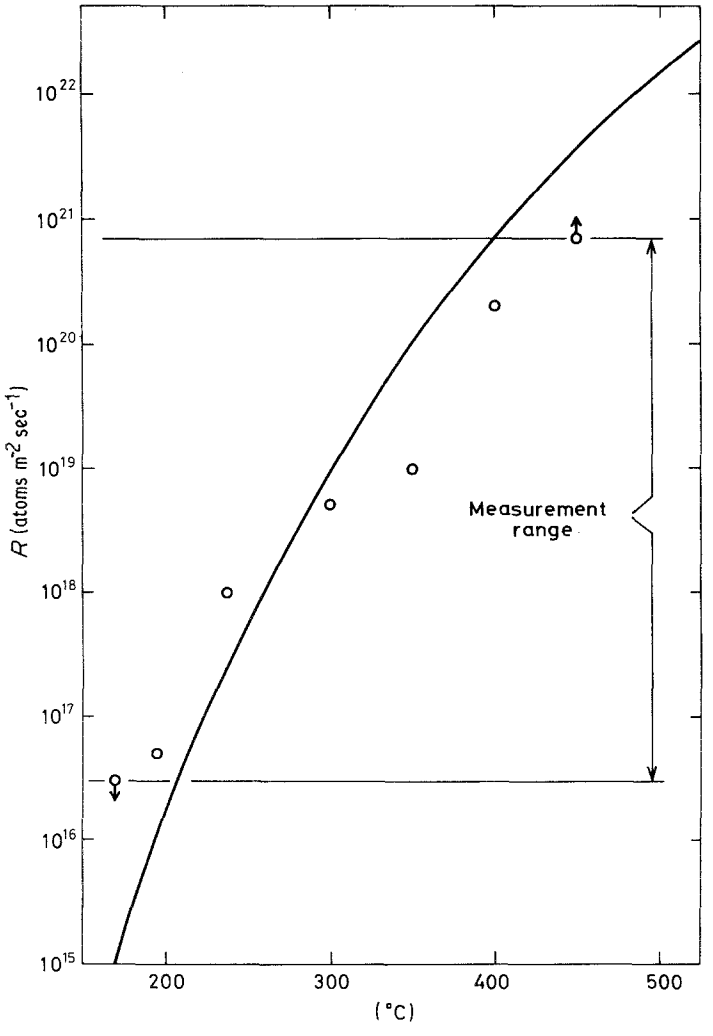

Figure 2 The rate of evaporation of magnesium from the Al–0.8Mg alloy as a function of temperature. The curve is that calculated from Equation 9.

the Auger electron technique in a total time of only 1 msec.

It is only in a fairly narrow temperature range, 100 to 300° C that curves of the form shown in Fig. 1 might be experimentally attainable. In this temperature range for the Al–0.8Mg alloy V lies between 5 and 20 and the maximum segregation level occurs within the practical range of measurement, 1 min to several hours. Before the theoretical curves of Fig. 1 can be compared with experimental meaurements of segregation levels and evaporation rates, the diffusivity of magnesium in aluminium must be ascertained. This was done by following the kinetics of the approach to segregation equilibrium at temperatures for which the evaporation rate is negligible.

5. The kinetics of segregation

5.1. The diffusion equation

Experimental measurements of the time dependence of magnesium segregation C_s^t may be fitted to Equation 6 and provided α is known and evaporation is negligible, the diffusion coefficient D can be found. In practice α is only constant at low segregation levels, and tends to fall, often quite rapidly, as segregation proceeds, thus continuously changing the time scale of Fig. 1 and consequently changing the shape of the segregation curve [5]. In the present case, however, of magnesium segregating from Al–Mg alloys, the segregation level remains sufficiently low for the enrichment factor α to be considered constant during the approach to equilibrium.

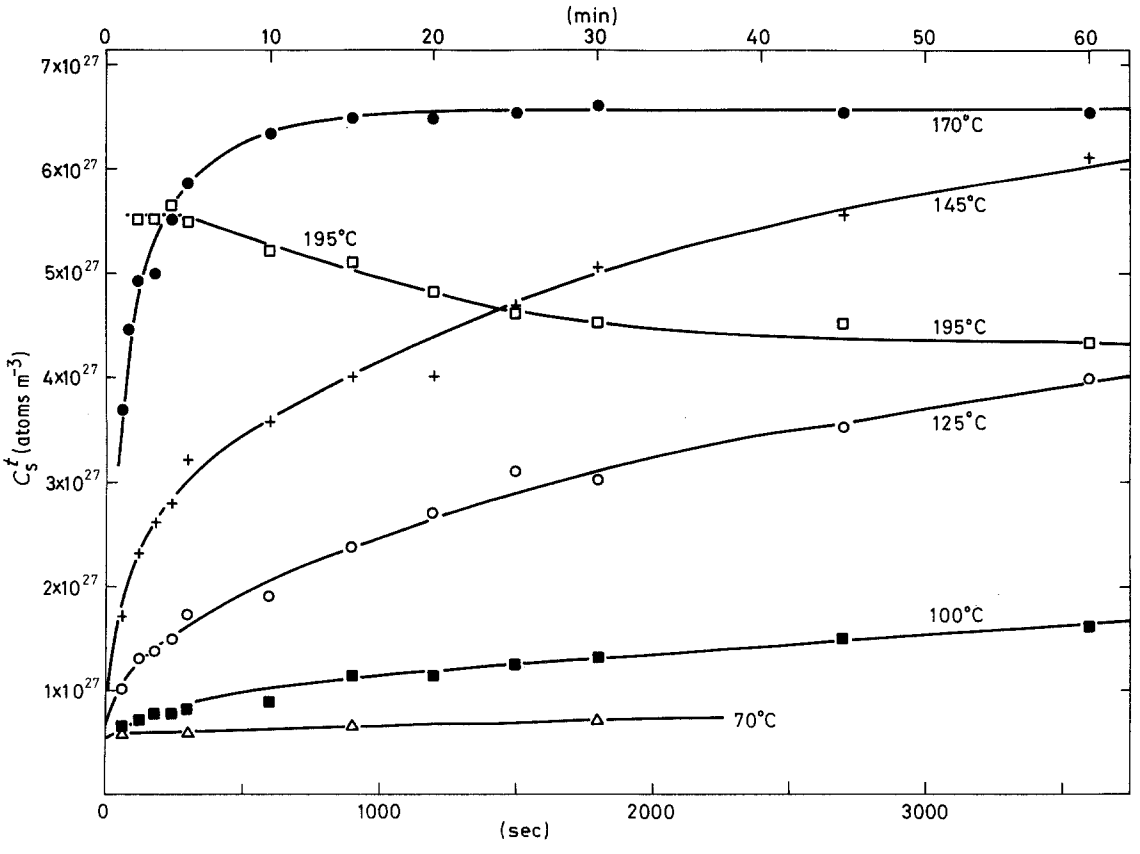

Figure 3 The magnesium concentration in the surface atomic layer of the Al–0.8Mg alloy as a function of time and temperature.

Equation 6, for short times, approximates to the infinite solid solution of Fick's second law [8]. This is because the surface mobility of the segregated magnesium is sufficiently high for the rate of magnesium mass flow across the imaginary bulk–surface interface to be described thus. Hence

$$\frac{C_s^t - C_s^0}{C_\infty - C_s^0} = \frac{2}{d}\left(\frac{Dt}{\pi}\right)^{1/2} \qquad (10)$$

Following other workers [9], the experimentally observed time dependence of the approach to equilibrium can be compared easily with the $t^{1/2}$ dependence predicted by Equation 10.

5.2. Surface segregation measurements

Measurements of the surface segregation of magnesium were made for the Al–0.8Mg alloy. Data of the kinetic approach to equilibrium were accessible only in the range 100 to 170° C. At lower temperatures, the extensive periods of heating resulted in significant contamination from prolonged outgassing of materials in the environs of the hot stage, while at higher temperatures the time for equilibrium surface segregation to be attained was of the same magnitude as the time for the specimen to attain the required temperature. Also, at temperatures in excess of 170° C the evaporation of magnesium as already discussed, became significant. During the period that magnesium was segregating, only the two peaks used to quantify the aluminium and the magnesium were monitored, but when an equilibrium segregation had been attained, entire spectra were recorded to confirm that no impurity segregation to the free surface had occurred.

The quantified surface segregation data, C_s^t are shown in Fig. 3 as a function of the time at temperature. At 195° C it can be seen that magnesium evaporation is significant and C_s^t is, in fact, observed to fall. At 170° C an equilibrium surface concentration of about 6.6×10^{27} atoms m^{-3} was reached after some 20 min. This is equivalent to about 15% of a close packed monolayer. The samples at 145 and 125° C were left at tempera-

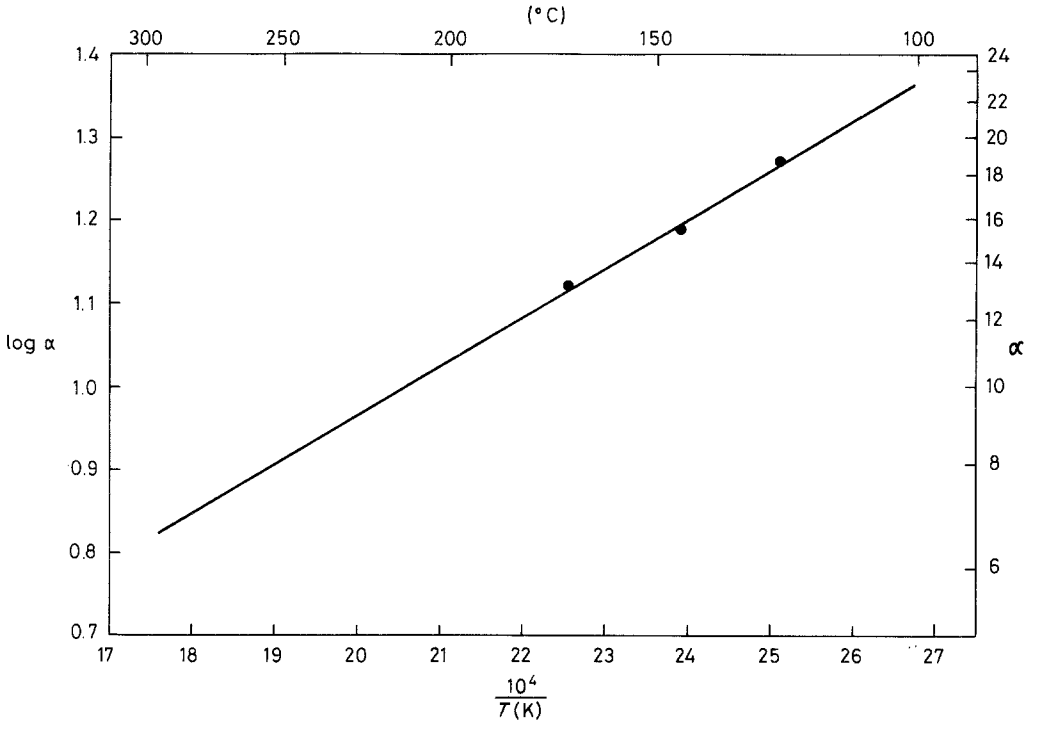

Figure 4 Measured values of the surface segregation enrichment ratio α for magnesium in the Al–0.8Mg alloy.

ture overnight and for 2 days, respectively, to attain segregation levels close to equilibrium. These were measured, as 7.5×10^{27} and 8.5×10^{27} atom m^{-3}, or about 17% and 20% of a monolayer, respectively. These three measurements are plotted in Fig. 4, in terms of values of enrichment ratio, α, from a bulk concentration of 5.4×10^{26} atoms m^{-3} of magnesium. Extrapolation of these data allows values for α to be estimated over the entire range of surface segregation measurements, namely 100 to 300° C, assuming an Arrhenius dependence upon the temperature, of the segregation level. Values of α in this temperature interval range from about 24 to 7.

Magnesium has been recently experimentally observed to enrich at grain boundaries in Al–Mg alloys to a level two or three times its concentration in the bulk [10]; this in material quenched from 350° C. Magnesium is also known to segregate to grain boundaries in Al–Zn–Mg alloys [11–13]. From work on other systems [14] it is generally expected that the enrichment of a segregant at a free surface will be somewhat greater than at a grain boundary; the precise ratio being dependent upon the vibrational, anharmonic and site-multiplicity effects on the entropy, and will be temperature dependent. Surface segregation levels can also be predicted [14–16] for binary alloys, for example in terms of the surface energies of the constituents, their enthalpy of mixing and the release of strain energy on segregation [16]. The prediction for the surface enrichment of magnesium in Al–Mg lies in the range 1 to 10.

Assuming the segregation layer thickness to be one atomic layer, such that d is 0.285 nm, the bulk diffusion coefficient has been determined from the slopes of the lines obtained by replotting the data at low times from Fig. 3 as a function of $t^{1/2}$ in Fig. 5. The data are in good agreement with the low time approximation given by Equation 10. The diffusional data have been plotted in Fig. 6 in the form of an Arrhenius plot, a least-squares fit to which gives a diffusivity for magnesium in the Al–0.8Mg alloy, in the temperature range 70 to 170° C of

$$D = 2.0 \times 10^{-6} \exp \frac{-117\,000}{RT} \text{ m}^2 \text{ sec}^{-1} \quad \text{(this study)} \qquad (11)$$

where R is 8.314 41 J mol^{-1} K^{-1}.

There are considerable data on solute and impurity diffusion in aluminium [17, 18] and those for magnesium in aluminium [18–40] have

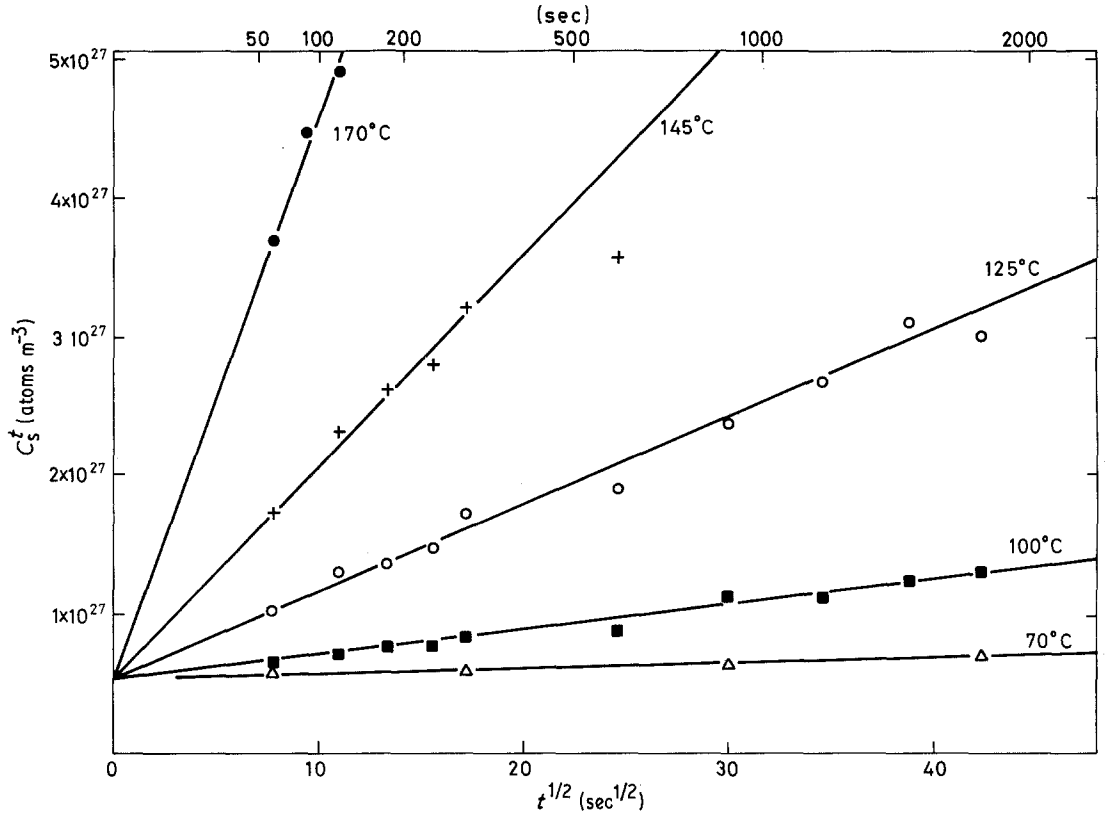

Figure 5 Surface segregation measurements of magnesium in the Al–0.8Mg alloy at low times and low temperatures in the regime of $t^{1/2}$ kinetics.

been compiled and shown by the circles in Fig. 7. The present work, shown by the crosses, extends the temperature range at the lower end to 70° C. The least squares fit to all the data in the figure is given by

$$D = 0.6 \times 10^{-6} \exp \frac{-125\,000}{RT} \text{ m}^2 \text{ sec}^{-1} \quad \text{(all data)}$$

5.3. Segregation and evaporation

We are now in a position to compare experimental measurements directly with the theoretical curves of Fig. 1. The time-dependent segregation levels C_s^t from quantified AES measurements are shown partially in Fig. 3, the surface enrichment ratio values, α, in the temperature range of interest, 100 to 300° C, can be extrapolated from the data in Fig. 4, and the diffusivity, D, can be obtained from Equation 11. Thus for each measurement of a segregation level the time, t, at temperature can be expressed in units of $\alpha^2 d^2/D$ and the level itself, C_s^t normalized to the equilibrium value that would be attained in the absence of evaporation. All the measurements taken are presented in this form in Fig. 8.

The experimental results are clearly of the form predicted in Fig. 1 and the mismatch in the data can be accounted for by uncertainty of the quantification of the AES, as well as the values of V, α and D.

The assumption by Sun *et al.* [41] that evaporation beats segregation kinetically at 300° C to explain their observed absence of magnesium segregation is shown to be correct. The kinetics of magnesium loss in vacuum are controlled by the bulk diffusion as shown by mass spectrometric studies [42] and are the same as when the Al–Mg is heated in air. In the first case the magnesium is lost by evaporation while in the second by a surface reaction [43]. In both situations it is the diffusivity of magnesium that is the controlling factor.

6. Heat-treatment in air

6.1. The oxidation of Al–Mg alloys

The oxidation of aluminium and its alloys with magnesium has been studied at length [1, 44–47].

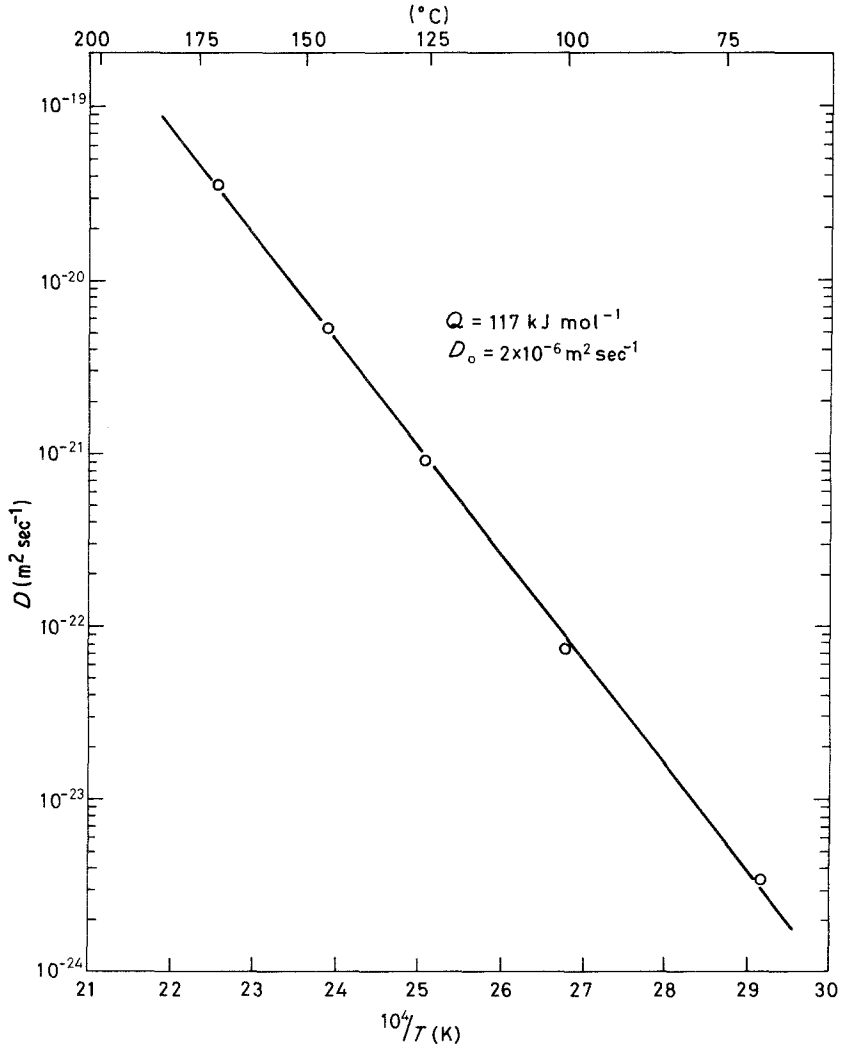

Figure 6 Diffusion measurements for magnesium in the Al–0.8Mg alloy in the temperature range 70 to 170° C.

In particular the oxidation of the two alloys of interest here, Al–0.8 Mg and Al–2.5 Mg in their production, as rolled state has been investigated recently [1]. Besides being of industrial importance, a knowledge of the mechanisms of oxidation are of interest because of the very different behaviour of the two pure components. During oxidation, pure aluminium has an initial parabolic oxide growth, transforming by way of several intermediate stages to one of decreasing rate such that a protective film of limiting thickness, dependent upon the temperature (200 nm at 550° C), is formed. On the other hand, the protective oxide film formed initially on pure magnesium is partially ruptured at about 400° C, leading to oxidation with linear kinetics and, above 550° C, complete rupture of the film with a much more rapid oxidation. The rate of oxidation of Al–Mg alloys depends upon the relative rates of diffusion of the two metals in the oxide film.

6.2. Experimental procedures

Polished coupons of both alloys were subjected to heat-treatments of up to 1 h in the temperature range up to 600° C in dry flowing air. The coupons were then mounted in the Auger electron spectrometer and composition depth profiles obtained, from the oxide–air surface through the oxide film and the depletion zone, into the virgin alloy. Ion sputtering of the oxide provides a concentration profile as a function of sputtering time. In order to quantify the sputtered depth it is necessary to known the incident ion flux and the sputter yield of the sample surface. The ion flux

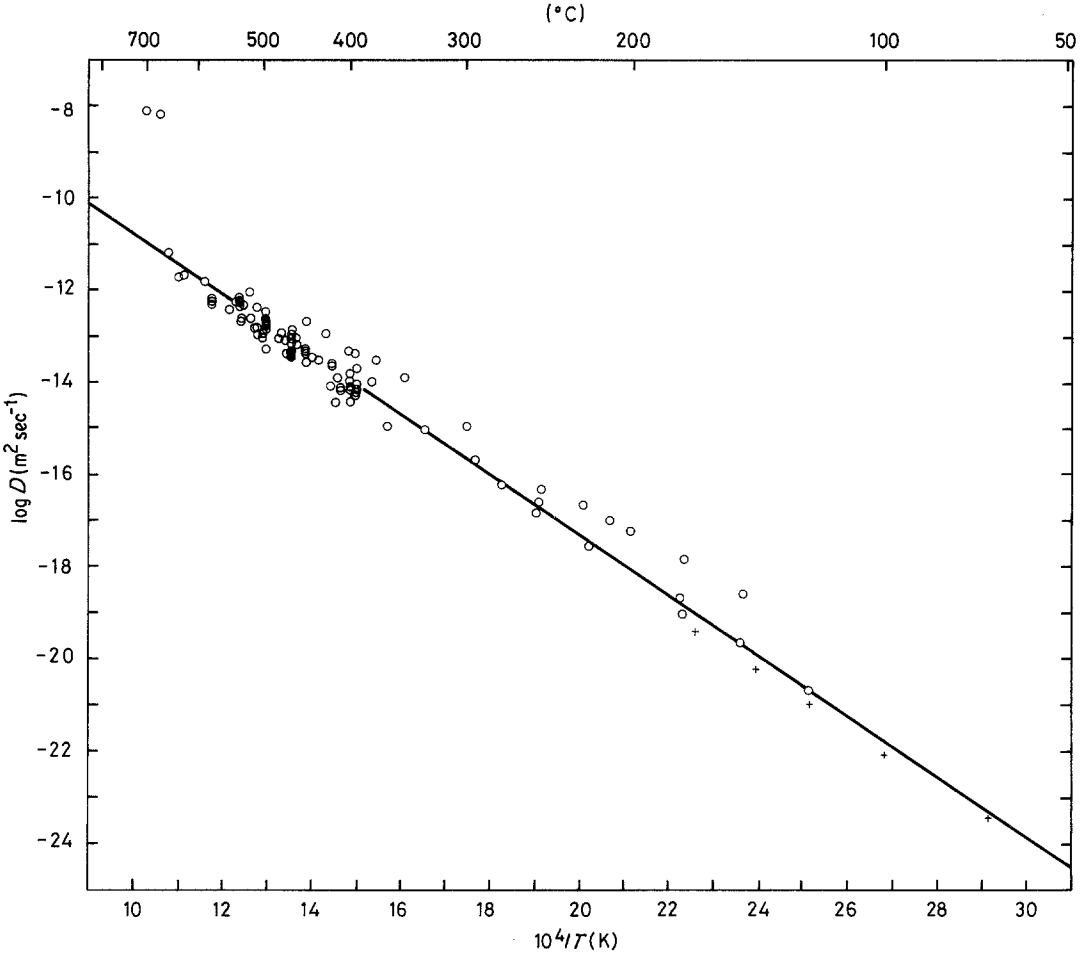

Figure 7 The diffusivity of magnesium in aluminium from data in [18–40]. The data in Fig. 6 are shown with the different symbol.

of the argon ion gun can be measured with a Faraday cup but the sputter yield is strongly dependent upon the species and its matrix and also probably varies during the sputtering of the oxide film. The interpretation and quantification of sputtered depth profiles using Auger electron spectroscopy has recently been reviewed [48].

On the sample which had had no heat-treatment, with a very thin, room temperature formed oxide film, the Al_{1396} peak became distinct from the Al^{3+}_{1380} peak after a few minutes of sputtering. From this point until the complete disappearance of the oxide peak, the intensity of the Al_{1396} peak, I_t, compared to its final maximum value, I_∞ is given by [2]

$$\frac{I_t}{I_\infty} = \exp \frac{-z_0}{\lambda \cos \theta} \qquad (12)$$

where z_0 is the thickness of the oxide film, λ is the imfp of the Al_{1396} Auger electrons and θ is the angle of collection of the electrons from the sample, here 42° for the cylindrical mirror analyser. In this way, using Equation 12 and sputtering through a very thin oxide film a sputtering rate of 42.5 nm h^{-1} was measured for the removal of the oxide consisting principally of Al_2O_3.

Sputtering rates were also measured using sampes with thick oxides of Al_2O_3 and MgO, formed at 600° C. The surfaces were partially masked with a tungsten shield while sputtering. The thickness of the material removed by the argon ion beam was determined using an interference microscope.

For Al_2O_3 a mean sputtering rate of 45 nm h^{-1} was measured while the corresponding figure for MgO was 39 nm h^{-1}. This confirms that magnesia is slightly more difficult to ion sputter than is alumina, as was shown by Bach [49] who measured

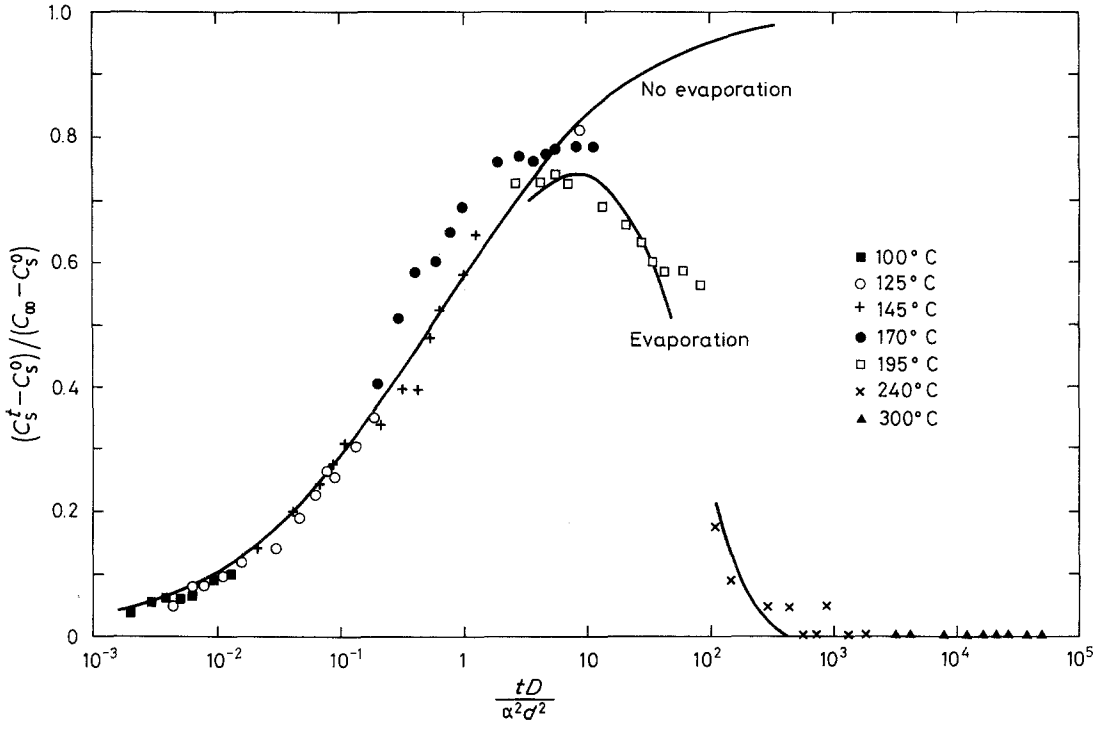

Figure 8 Surface segregation measurements of magnesium on the Al–0.8Mg alloy plotted in the form of the universal segregation–evaporation curves of Fig. 1.

sputtering yields, with 5 keV argon ions, of 0.82 and 0.9 atoms/ion, respectively.

6.3. Concentration–depth profiles

All the concentration–depth profiles through the oxides exhibited a similar form which is shown in an idealized way in Fig. 9. The Auger electron spectra have been quantified in terms of atomic percentages and the symbols Al and Mg represent the atomic concentrations of the metals whilst Al^{3+} and Mg^{2+} represent the atomic concentrations of these elements in their oxide state.

On all the composition–depth profiles aluminium metal coexists with alumina and magnesia over a large proportion of the oxide thickness. Thus, the precise depth at which the oxide–metal

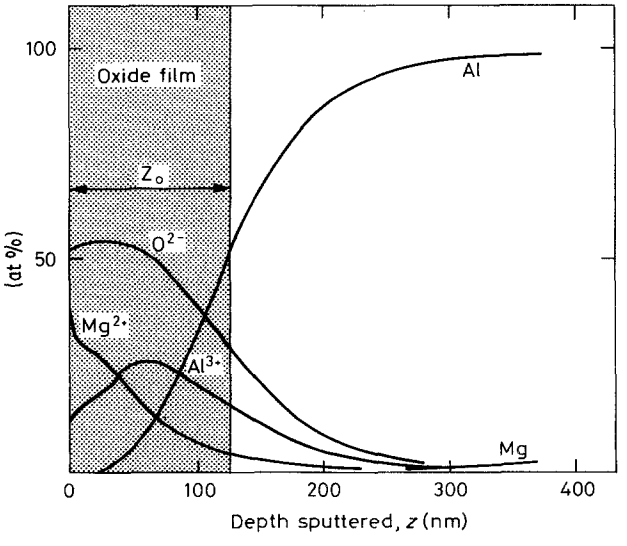

Figure 9 A typical quantified compositon–depth profile through an oxidized sample of an Al–Mg alloy. The oxide–metal interface is defined as the depth when aluminium is 50 at %.

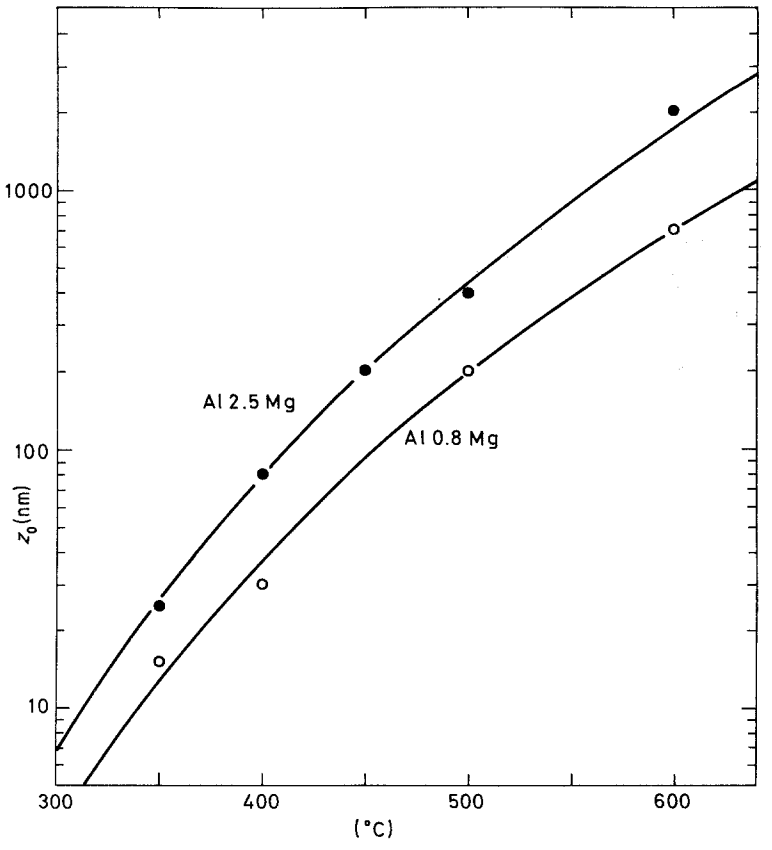

Figure 10 The oxide thickness variation with temperature in the range 300 to 600° C after a 1 h heat treatment in dry flowing air.

interface exists cannot be unambiguously defined. In the present case the thickness of the oxide layer, z_0 is taken as the mean depth sputtered at which the aluminium signal, Al, has risen to 50 at%. This depth is also close to that at which the O^{2-} signal is half of its value in the oxide. This is as indicated in Fig. 9.

The temperature dependence of oxide thickness in the range 300 to 600° C is shown in Fig. 10, the data obtained from depth profiling of samples heated for 1 h at temperature in dry flowing air. It is possible to calculate the diffusion coefficient of magnesium in the oxide film by assuming that this is the process controlling the growth of the surface oxide. The concentration of magnesium at the oxide–metal interface is constant and equal to the volume concentration, since ion sputtering reveals no depletion layer below the oxide. Also, the external oxidation is very rapid and the diffusion of oxygen into the oxide is essentially zero. The only further assumption is that the concentration gradient of magnesium through the oxide is approximately linear which, to a first approximation is shown to be so in the concentration–depth profiles. Hence the solution to Fick's law for the magnesium flux

$$J_{Mg} = -D\frac{\partial C_z}{\partial x} \tag{13}$$

is given by

$$z_0^2 C_s = 2DC_\infty t \tag{14}$$

relating the oxide thickness, z_0, and the time of oxidation, t. D is the diffusion coefficient of the magnesium through the oxide, C_∞ the bulk concentration of magnesium in the alloy and C_s the concentration of magnesium at the oxide surface. Hence

$$2\ln z_0 = -\frac{Q}{RT} + \ln\frac{2D_0 C_\infty t}{C_s} \tag{15}$$

and the data presented in Fig. 10 has been replotted in Fig. 11 to show that $\ln z_0$ is indeed inversely proportional to the temperature T as predicted from Equation 15. Furthermore, Equation 15 may be used to calculate the acti-

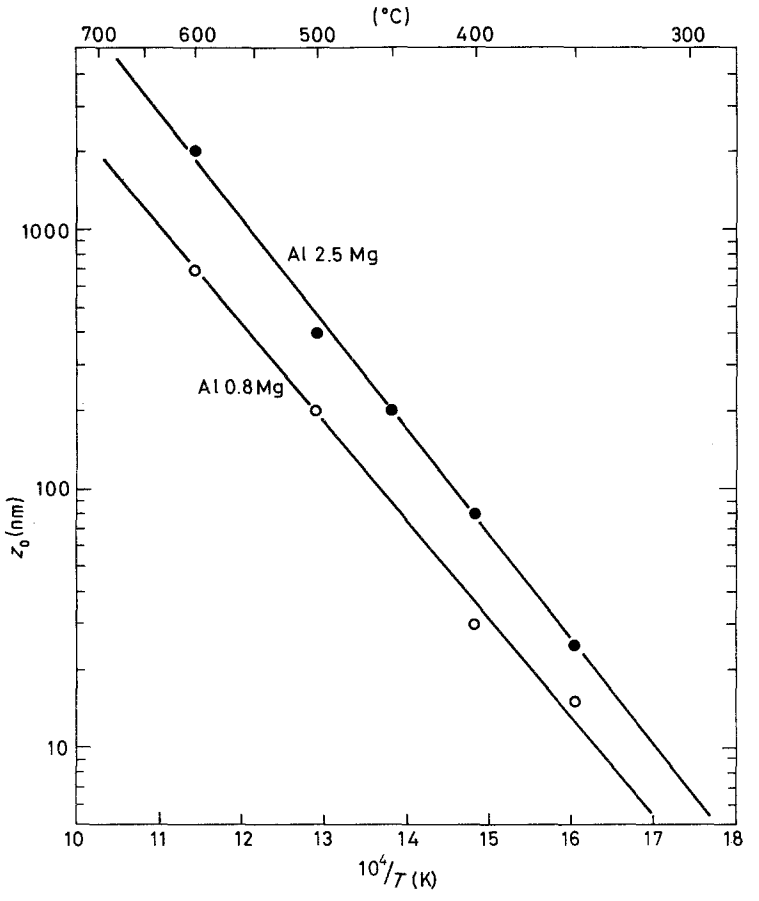

Figure 11 An experimental test of Equation 15 for oxide film thickness after a 1 h heat treatment in dry flowing air in the temperature range 300 to 600° C.

vation energy for diffusion at each temperature, which should be largely independent of the alloy composition. These data are given in Fig. 12 from which the least squares fit gives a diffusion coefficient D:

$$D = 1.0 \times 10^{-6} \exp \frac{-150\,000}{RT} \text{ m}^2 \text{ sec}^{-1}$$

(this study) (16)

where $R = 8.31441 \text{ J mol}^{-1} \text{ K}^{-1}$.

Several measurements have been made of the diffusivity of magnesium in its oxide [50–54]. These are presented by the circles in Fig. 13 and described by:

$$D = 4.4 \times 10^{-8} \exp \frac{-234\,000}{RT} \text{ m}^2 \text{ sec}^{-1}$$

(all other data).

The variation in these data is thought to be due to impurities in the magnesia [55]; the lower limit of diffusion coefficient being for pure material [53] while the upper limit is for material with about 0.2% impurities [51].

Diffusion of magnesium in the thin oxide films would be expected to be some 100 times greater than in the magnesia single crystals because of grain-boundary diffusion. The small grain size of the oxide film enables about 10% to be grain boundaries. The difference increases as the temperature decreases since the activation energy is only two-thirds of that for the lattice. This factor is quite typical of that generally found to relate the activation energies for grain boundaries and the lattice [56]. Furthermore, in the present work, D_{gb} is measured as the film grows, so there is no potential barrier at the metal–oxide interface and material can be carried across that interface very readily resulting in a diffusivity which may be many orders of magnitude higher than for the stoichiometric crystal lattice.

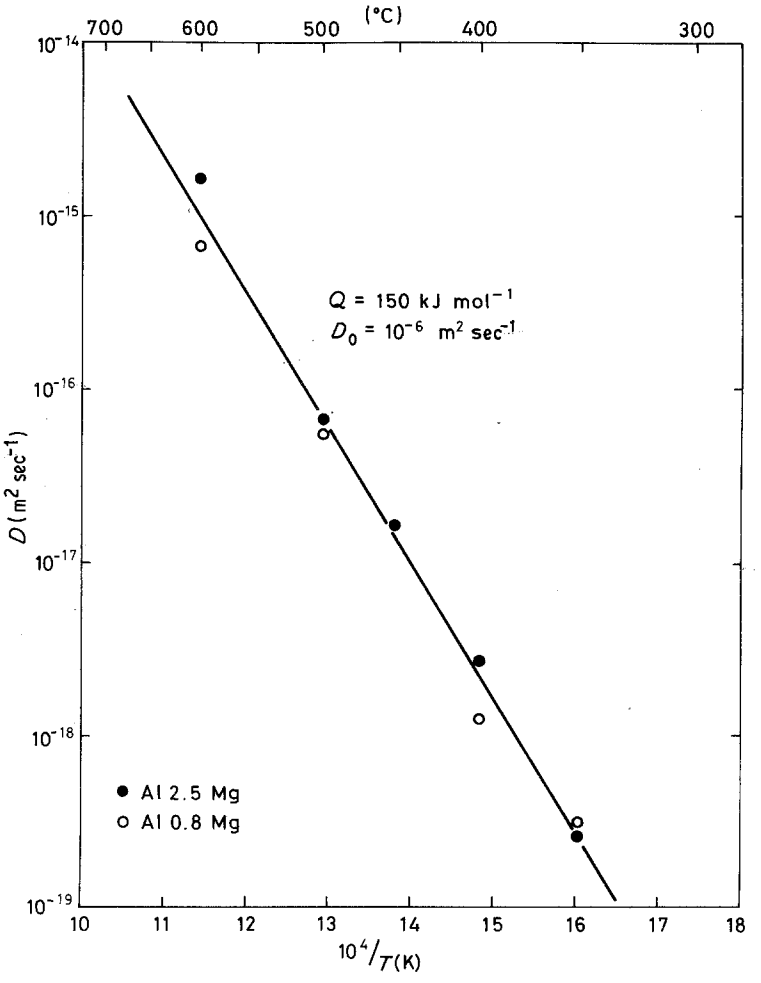

Figure 12 The diffusivity of magnesium in oxide films grown on Al–Mg alloys.

7. Conclusions

The combination of the competing processes of surface segregation and evaporation has been treated theoretically and compared with Auger electron spectroscopic measurements of the kinetics of surface segregation and of evaporation rates in the Al–Mg system, in the temperature range up to 600° C. In broad terms the agreement is very good indicating that the mechanisms of diffusion segregation and evaporation are understood.

The surface enrichment at equilibrium has been found to be about 24 at 100° C falling to about 12 at 200° C. At temperatures above 200° C the evaporation rate exceeds the segregation kinetics and the magnesium enrichment rises to a maximum before falling to zero. The maximum level occurs after about 4 min at 200° C and about 200 msec at 300° C. Thus a surface enrichment at temperatures above about 250° C is not, in practice, observed.

The diffusivity of magnesium in aluminium in the range 70 to 170° C has been determined from the segregation data and is in excellent agreement with the existing data taken at higher temperatures, all of which are compiled here.

The same Al–Mg alloys heat-treated in vacuum, have also been heat-treated in dry air in the temperature range up to 600° C. The oxide films have been composition–depth profile using Auger electron microscopy with ion sputtering and the diffusivity of magnesium in the growing oxide films determined from the oxidation kinetics. These data are compared with existing data taken on bulk oxide samples.

Acknowledgements

The authors would like to thank Dr Jon Ball of

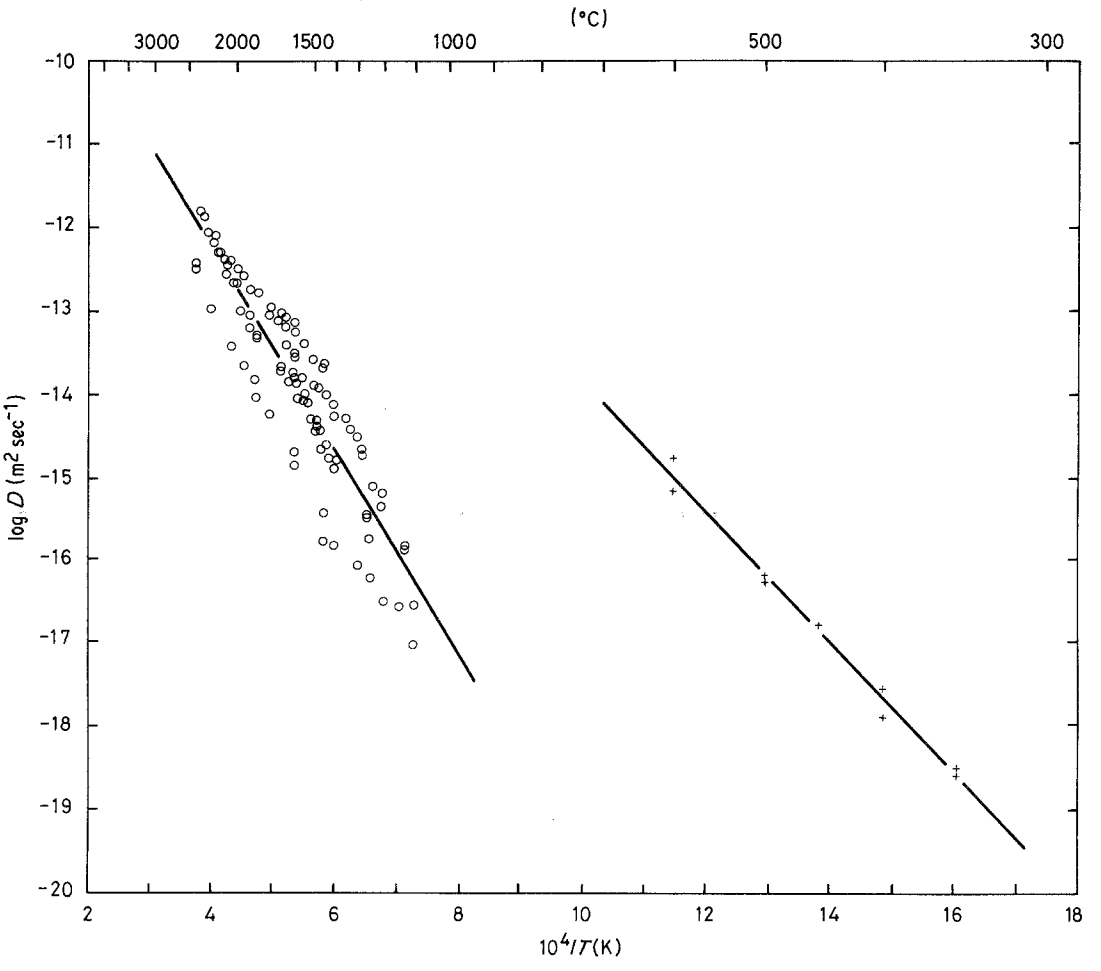

Figure 13 A compilation of diffusivity data [50–54] for magnesium in bulk magnesium oxide. The crosses are the data from Fig. 12 for the diffusivity of magnesium in a growing oxide thin film.

British Alcan Aluminium for providing the sample material, and Dr Martin Seah of the National Physical Laboratory for his critical involvement in the work.

References

1. C. LEA and J. BALL, *Appl. Surf. Sci.* **17** (1984).
2. M. P. SEAH and W. A. DENCH, *Surf. Interface Anal.* **1** (1979) 2.
3. M. P. SEAH, *Analusis* 9 (1981) 171.
4. S. ICHIMURA and R. SHIMIZU, *Surf. Sci.* **112** (1981) 386.
5. C. LEA and M. P. SEAH, *Phil. Mag.* **35** (1977) 213.
6. S. DUSHMAN, "Scientific Foundations of Vacuum Technique", 2nd Edn (John Wiley, 1962).
7. R. E. HONIG and D. A. KRAMER, *RCA Review* **30** (1969) 285.
8. J. CRANK, 'The Mathematics of Diffusion" (Clarendon Press, Oxford, 1956).
9. S. HOFMANN and J. ERLEWEIN, *Scripta Metall.* **10** (1976) 857.
10. T. MALIS and M. C. CHATURVED, *J. Mater. Sci.* **17** (1982) 1479.
11. R. L. EDGAR, *Canad. Metall. Q.* **13** (1974) 177.
12. J. M. CHEN, T. S. SUN, R. K. VISWANADHAM and J. A. S. GREEN, *Met. Trans.* **8A** (1977) 1935.
13. T. S. SUN, J. M. CHEN, R. K. VISWANADHAM and J. A. S. GREEN, *Appl. Phys. Lett.* **31** (1977) 580.
14. H. P. STUWE and I. JAGER, *Acta. Metall.* **24** (1976) 605.
15. J. J. BURTON and E. S. MACHLIN, *Phys. Rev. Lett.* **37** (1976) 1433.
16. M. P. SEAH, *J. Catalysis* **57** (1979) 450.
17. J. W. H. CLARE, *Metallurgia* **57** (1958) 273.
18. M. BISHOP and K. E. FLETCHER, *Int. Met. Rev.* **17** (1972) 203.
19. H. R. FRECHE, *Trans. AIME* **122** (1936) 324.
20. R. M. BRICK and A. PHILLIPS, *ibid.* **124** (1937) 331.
21. N. A. BELOSERSKI, *Legkije Metally (Light Metals)* **6** (10) (1937) 18.
22. W. BUNGARDT and F. BOLLENRATH, *Z. Metallkde.* **30** (1938) 377.

23. K. UEMARA, *Tetsu-to-Hagane* **25** (1939) 24.
24. *Idem, ibid.* **26** (1940) 813.
25. A. BEERWALD, *Z. Electrochem.* **45** (1939) 789.
26. W. BUNGARDT and H. CORNELIUS, *Z. Metallkde.* **32** (1940) 360.
27. R. F. MEHL, F. N. RHINES and K. A. VON DEN STEINEN, *Metals and Alloys* **13** (1941) 41.
28. H. BÜCKLE, *Z. Elektrochem.* **49** (1943) 238.
29. M. RENOUARD, *Rev. Metall.* **48** (1951) 944.
30. P. G. SHEWMON and F. N. RHINES, *Trans. AIME* **200** (1954) 1021.
31. P. G. SHEWMON, *ibid.* **206** (1956) 918.
32. T. AMITANI, *Sumito Light Metal Tech. Rep.* **1** (1960) 123.
33. W. ROTH, *Metall.* **14** (1960) 979.
34. S. Z. BOKSHTEIN, M. B. BRONFIN, S. T. KISHKIN and V. A. MARICHEV, *Metall. Termicheskaya Obrabotka Metallov* **4** (1965) 36.
35. H. Y. HUNSICKER, "Aluminium", Vol. 1 (American Society for Metals, Cleveland, Ohio, 1967) p. 118.
36. A. J. CORNISH and M. K. B. DAY, *J. Inst. Metals* **97** (1969) 44.
37. P. DOIG and J. W. EDINGTON, *Phil. Mag.* **28** (1973) 961.
38. P. DOIG, J. W. EDINGTON and G. HIBBERT, *ibid.* **28** (1973) 971.
39. P. DOIG and J. W. EDINGTON, *ibid.* **29** (1974) 217.
40. S. ROTHMAN, N. L. PETERSON, L. J. NOWICKI and L. C. ROBINSON, *Phys. Status Solid* **B63** (1974) K29.
41. T. S. SUN, J. M. CHEN, R. K. VISWANADHAM and J. A. S. GREEN, *J. Vac. Sci. Technol.* **16** (1979) 668.
42. E. HIDVÉGI and E. KOVÁCS-CSETÉNYI, *Mat. Sci. Eng.* **27** (1977) 39.
43. I. KOVÁCS, J. LENDVAI and T. UNGÁR, *ibid.* **21** (1975) 169.
44. W. W. SMELTZER, *J. Electrochem. Soc.* **103** (1956) 209.
45. R. A. HINE and R. D. GUMINSKI, *J. Inst. Metals* **89** (1961) 417.
46. C. N. COCHRAN and W. C. SLEPPY, *J. Electrochem. Soc.* **108** (1961) 322.
47. P. E. BLACKBURN and E. A. GULBRANSEN, *ibid.* **107** (1960) 944.
48. C. LEA, *Met. Sci.* (1983) 357.
49. H. BACH, *Nucl. Instrum. Meth.* **84** (1970) 4.
50. R. LINDNER and G. D. PARFITT, *J. Chem. Phys.* **26** (1957) 182.
51. B. C. HARDING, D. M. PRICE and A. J. MORTLOCK, *Phil. Mag.* **23** (1971) 399.
52. B. C. HARDING and D. M. PRICE, *ibid.* **26** (1972) 253.
53. B. J. WUENSCH, W. C. STELLE and T. VASILOS, *J. Chem. Phys.* **58** (1973) 5258.
54. M. DUCLOT and C. DEPORTES, *J. Solid State Chem.* **31** (1980) 377.
55. D. R. SEMPOLINSKI and W. D. KINGERY, *J. Amer. Ceram. Soc.* **63** (1980) 664.
56. D. MCLEAN, "Grain boundaries in metals" (Oxford University Press, London, 1957).

Received 13 July
and accepted 4 October 1983